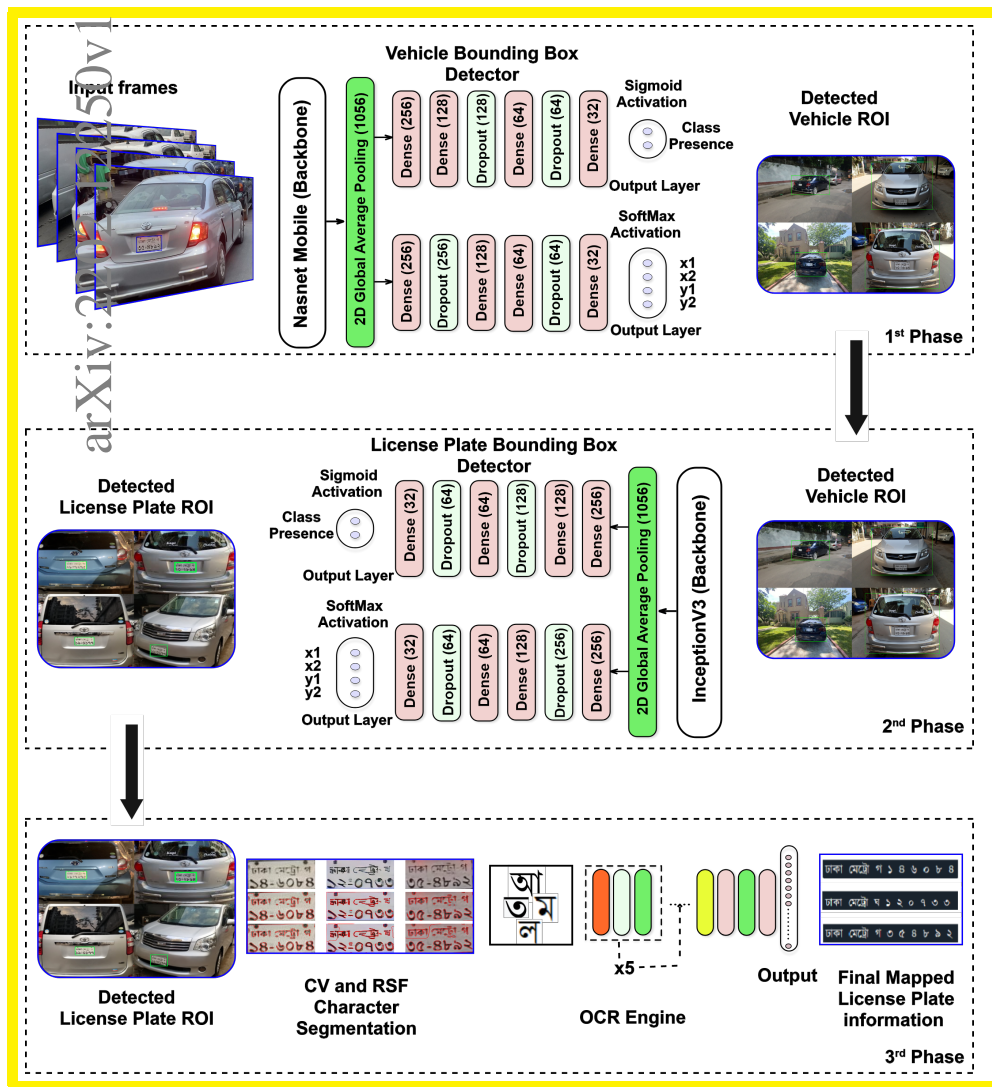


# Graphical Abstract

## BLPnet: A new DNN model and Bengali OCR engine for Automatic License Plate Recognition

Md. Saif Hassan Onim, Hussain Nyeem, Koushik Roy, Mahmudul Hasan, Abtahishmam, Md. Akiful Hoque Akif, Tareque Bashar Ovi



## Highlights

### **BLPnet: A new DNN model and Bengali OCR engine for Automatic License Plate Recognition**

Md. Saif Hassan Onim, Hussain Nyeem, Koushik Roy, Mahmudul Hasan, Abtahi Ishmam, Md. Akiful Hoque Akif, Tareque Bashir Ovi

- We propose an end-to-end Deep Neural Network (DNN) model that we call BLPnet for real-time Automatic License Plate Recognition (ALPR) system.
- BLPnet is proposed to operate in two separate detection phases to eliminate the false positive detection of number plate.
- BLPnet also captures a lower set of trainable parameters adequate for the vehicle license plate detection, and thus, its potential for the real-time application is confirmed with its impressive computational efficiency compared to the prominent ALPR systems.
- A new Convolutional Neural Network (CNN) based OCR engine is developed for rotation invariant Bengali license plate's character recognition and information retrieval with notably higher accuracy.

# BLPnet: A new DNN model and Bengali OCR engine for Automatic License Plate Recognition

Md. Saif Hassan Onim, Hussain Nyeem, Koushik Roy, Mahmudul Hasan,  
Abtahi Ishmam, Md. Akiful Hoque Akif, Tareque Bashar Ovi

<sup>a</sup>*Department of EECE, Military Institute of Science and Technology (MIST), Mirpur  
Cantonment, Dhaka, 1216, , Bangladesh*

---

## Abstract

The development of the Automatic License Plate Recognition (ALPR) system has received much attention for the English license plate. However, despite being the sixth largest population around the world, no significant progress can be tracked in the Bengali language countries or states for the ALPR system addressing their more alarming traffic management with inadequate road-safety measures. This paper reports a computationally efficient and reasonably accurate Automatic License Plate Recognition (ALPR) system for Bengali characters with a new end-to-end DNN model that we call Bengali License Plate Network(BLPnet). The cascaded architecture for detecting vehicle regions prior to vehicle license plate (VLP) in the model is proposed to eliminate false positives resulting in higher detection accuracy of VLP. Besides, a lower set of trainable parameters is considered for reducing the computational cost making the system faster and more compatible for a

---

*Email addresses:* saif@eece.mist.ac.bd (Md. Saif Hassan Onim),  
h.nyeem@eece.mist.ac.bd (Hussain Nyeem), rkoushikroy2@gmail.com (Koushik  
Roy), mahmud108974@gmail.com (Mahmudul Hasan), abtahiishmam3@gmail.com  
(Abtahi Ishmam), mohammadaxif5717@gmail.com (Md. Akiful Hoque Akif),  
ovitareque@gmail.com (Tareque Bashar Ovi)

real-time application. With a Computational Neural Network (CNN)based new Bengali OCR engine and word-mapping process, the model is characters rotation invariant, and can readily extract, detect and output the complete license plate number of a vehicle. The model feeding with 17 frames per second (fps) on real-time video footage can detect a vehicle with the Mean Squared Error (MSE) of 0.0152, and the mean license plate character recognition accuracy of 95%. While compared to the other models, an improvement of 5% and 20% were recorded for the BLPnet over the prominent YOLO-based ALPR model and the Tesseract model for the number-plate detection accuracy and time requirement, respectively.

*Keywords:* ALPR, CNN, INCEPTION-V3, License plate detection, NASNet Mobile, OCR

---

## 1. Introduction

Automatic License Plate Recognition (ALPR) systems have received much attention to modern transportation services mainly for automatic management of traffic, parking, toll-station, and other road operations including surveillance and recognition of potential threats [1]. An ALPR system consists of three main phases: *frame-selection*, *character-segmentation*, and *optical character recognition* (OCR). The first phase verifies the existence of any Vehicle License Plate (VLP) in the input frame by extracting any possible character's features from the frame. The second phase separates the characters from the background followed by their recognition in the last phase. Such a system has more potential for the developing countries or states requiring higher road-safety measures and better traffic management.

One such potential group of the developing regions is the Bengali speaking countries and states that still requires a promising ALPR system for the Bengali VLP application. Unlike English characters, Bengali has more complex features leaving its accurate recognition from a VLP more challenging. Despite being the six largest population around the world [2], no significant progress can be tracked in the Bengali language countries or states for the ALPR system addressing their inadequate road-safety measures and poor traffic management. Besides, the performance of the prominent ALPR models developed for the English VLP is also unknown for the Bengali VLP recognition application.

Recent ALPR systems for English VLP captures the employment of promising machine learning models. Such models mainly detects the VLP in the given image (or a video frame) followed by the recognition of the text information on the plate. A variety of models are stemmed from the need for improving the classification accuracy, robustness to environmental artifacts, and computational efficiency. For example, the Convolutional Neural Network (CNN) based bounding box detectors were developed with regression algorithms [3, 4, 5, 6, 7], manual annotation [8], and transfer learning [9]. Other development with recurrent neural network (RNN) based architectures include the Bidirectional Long short-term memory (BiLSTM) based models [10], and real-time object detection algorithm, YOLO (You Only Look Once) and its variants based models [11, 12, 13]. The end-to-end cascaded and unified architectures of the neural networks were also studied for the ALPR systems [14, 15, 16, 17].

However, Unlike the English VLP, the effort in developing the ALPR

systems for the Bengali VLP is particularly limited. Despite much interest in developing Bengali handwriting, scripts and character recognition in general, it has not captured the ALPR system yet. A few notable developments of the ALPR systems for the Bengali VLP include the feature extraction based on the digital curvelet transform [18], Tesseract OCR [19], and CNN with Adam optimizer [20].

In summary, no Deep Neural Networks (DNN) model can be tracked in the literature that can detect the Bengali VLP and recognize its characters simultaneously. A few models only focused on the Bengali characters recognition [19, 20], but their performance is unknown for ALPR system. Although Tesseract and BornoNet have relatively high character recognition accuracy, they are not suitable for real-time applications like ALPR due to higher processing time. Unlike the above models, Onim *et al.* [17] recently combined YoloV4 for detection of VLP, and Tesseract as OCR engine. However, the model requires reasonably higher time for number plate detection and character recognition. All these mean that the models developed for either Bengali VLP detection or Bengali characters recognition are generally limited with *low detection and recognition accuracy*, and *high computational complexity* making them unsuitable for a real-time application.

In this paper, we, therefore, report an ALPR system with a new DNN model that we call Bengali License Plate Network (BLPnet) (Sec. 3). BLPnet is constructed to have three primary phases. Particularly, the contributions with the proposed three-phase ALPR system can be summarized as follows:

- Building on the NASNet-Mobile backbone architecture, the first phase employs more *dense* and *pulling* layers on the network-head to identify

the vehicles more efficiently with a region of interest bounding-box (Sec. 3.1).

- The second phase includes an InceptionV3 architecture customized with several *dense* and *pulling* layers to detect the VLP in the bounding-box region (Sec. 3.2).
- The third phase introduces a new Bengali-OCR engine (Sec. 3.3). Unlike the existing ALPR systems that cannot adequately tackle the artifacts like motion-blur and non-uniform shadow, the proposed engine employs de-blurring and Region Scalable Fitting (RSF) based segmentation, which are optionally invoked (*i.e.*, when characters are not recognized) to better tackle the intensity inhomogeneity.
- Additionally, detecting vehicle regions (first phase) prior to VLP (second phase), as considered in the proposed ALPR system, would significantly reduce computational cost and false-positives making the system faster and more accurate.

## 2. Related ALPR Systems

Development of several prominent ALPR systems for English VLP can be tracked in the literature so far. Getting the VLP information requires the localization and detection of the VLP. In CNN based approach, features are extracted for VLP and then object localization is done with bounding box detectors and regression algorithms [4, 6]. Silva *et al.* [7] and Laroca *et al.* [5] used bounding box regression to localize the object of interest with image coordinates using YOLO. These are One-stage detection networks and

relatively faster than other detectors. But these approach is computationally inefficient as it requires training *darknet* backbone of over  $27M$  parameters.

Alternatively, VLP can also be semantically segmented using a either CNN or deep segmentation network. Bulan *et al.* [3] proposed a real-time complete CNN model having higher adaptability to tackle the scene-variations requiring minimum possible human-intervention. An image-based classification was proposed with weak-Snow and strong-CNN classifiers. The first classifier was initially used for the region-tagging of the possible number-plates, and the strong-CNN refined the classification outputs for the actual number-plates Zhuang *et al.* [8] proposed such method where they segmented the VLP and the characters in it. This approach also needs a manual annotation of a characters and LP. Besides these segmentation based networks, segmentation free Networks have also been proposed. Wang *et al.* [6] proposed a convolutional Recurrent Neural Network (CRNN) and proposed a multi-task license plate detection and recognition (MTLPR) model. Zou *et al.* [10] used Bi-LSTM and directly localized characters without segmentation.

Both end-to-end cascaded and unified architectures have been used for ALPR system. Li *et al.* [16] used end-to-end trainable LP detection model that remains error-prone to the challenging conditions and also depends heavily on architectural design. On the other hand, cascaded architectures have the flexibility of tuning and testing. Hsu *et al.* [14] and Montazzolli *et al.* [15] proposed cascaded architecture for real time VLP detection and recognition.

Huang *et al.* [9] introduced Transfer learning into their CNN model to tackle the limited labeled data for a high detection accuracy of VLP of 93%. Later, with a modified YOLOv3 model with 10 CNNs, Chen *et al.* [11]

attempted to detect and recognize the VLP with an accuracy of about 98% and 78%, respectively in a variety of conditions (*i.e.*, rainy backgrounds, darkness and dimness, and varied colors and saturation of photos). In addressing several other environmental artifacts like poor-contrast and noisy images resulting from foggy, distortion and dusty conditions, Al-Shemarry *et al.* [12] improved the accuracy of VLP detection using a binary descriptor with contrast enhancement, leaving their proposed system limited to real-time application with poor frame-rate and higher computational cost. To tackle the motion artifacts (*i.e.*, blurry input images), Zou *et al.* [10] recently proposed a Bi-LSTM model with robust blur-kernel estimation that offered a reasonably lower accuracy of 79.55%. Another recent development with object bounding-box detection for ALPR system is YOLOv4 model [13], which is a deep convolutional network that can localize VLPs with immense frame rate and high accuracy.

Besides, on Bengali character detection and recognition, Majumdar *et al.* [18] proposed a feature extraction based on the digital curvelet transform. Separate  $k$ -nearest neighbor classifiers were trained using the curvelet coefficients of an original image and its morphologically changed copies. The overall recognition accuracy of 96.8% was reported while trained for twenty popular Bengali fonts and tested for different font sizes. Later, Hasnat *et al.* [19] attempted to successfully introduce Bengali script in Tesseract OCR. Tesseract can learn new languages or alphabets with training along with existing languages for character recognition. Recently, Rabby *et al.* [20] presented a new 13-layer CNN model called BornoNet for Bengali characters recognition. The model was designed with two sub-layers optimized using

adam optimizer Despite having relatively higher accuracy in the models for Bengali characters recognition, their applications to an ALPR system is not yet studied. In addressing the potential gap of having a promising ALPR system for Bengali VLP, we therefore develop and present real-time End-to-End DNN based model that we call BLPnet.

### **3. A New ALPR System with BLPnet**

This section presents a newly developed BLPnet model for ALPR system. As illustrated in Fig. 1, the model consists of three main phases that are cascaded together to detect vehicle, VLP and recognize the characters in it. It takes real-time video frames as input consisting of vehicles and its surroundings. In the first phase, the vehicle region is detected and distinguished using a bounding-box as the smallest possible rectangle with vertical and horizontal sides that entirely surround the vehicle captured in a frame. The frames containing the bounding boxes are fed to the VLP detection model along with the coordinates of the bounding-box. Later, the second phase detects and extracts the VLP contour followed by the character localization and recognition in the final phase. Consideration of intensity-inhomogeneity resilient segmentation and effective deployment of these cascaded modules would reduce the computational cost and false-positive predictions improving the accuracy and reliability of the system for a real-time application. These phases are now discussed below with more technical details.

#### *3.1. An Extended Vehicle Bounding-Box Detector*

A NASNet-Mobile is extended and used as the backbone of our DNN followed by six hidden layers to improve the vehicle detection accuracy (see

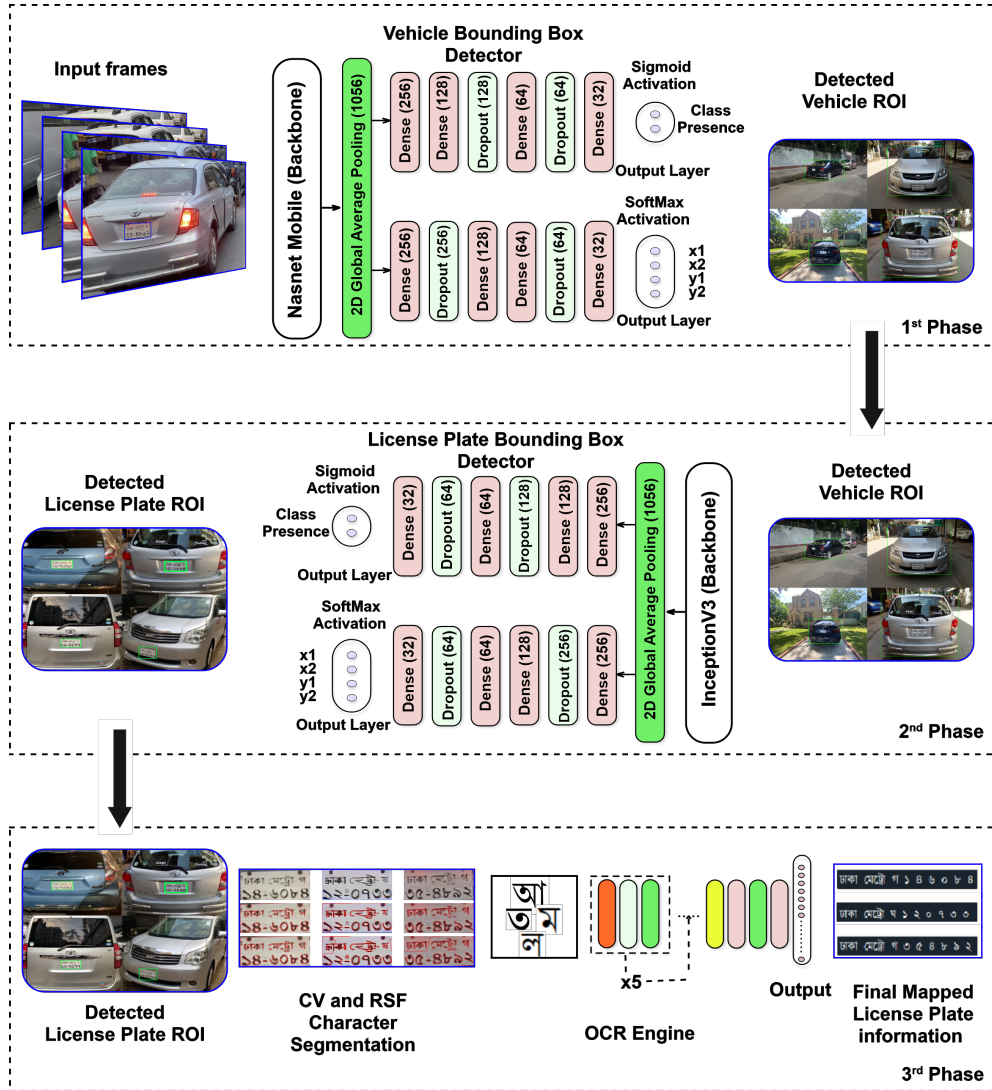


Figure 1: Key processes of the proposed ALPR system

Fig. 2). The NASNet-Mobile is more computationally efficient than its counterpart like the ResNet-based architecture that needs higher hardware configuration, making it unsuitable for large-scale deployment [21]. Thus, our model can be implemented on Field-Programmable Gate Array (FPGA) and other embedded devices to balance between hardware resources and processing speed. The TensorFlow (TF) v2.4 framework was used for the overall construction of our CNN model. The backbone was pre-trained with the Imagenet dataset [22]. Three hidden layers added as network head were fully connected layers followed by a dropout layer. A few important processing and considerations are briefly discussed below.

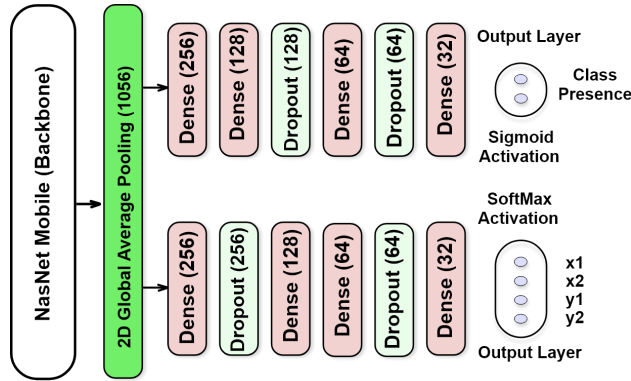


Figure 2: Vehicle Bounding-box detector of the proposed ALPR system

*Dataset Collection.* For the training of vehicle bounding-box detection model, we used the Cars dataset [23] of Stanford AI Lab. There are 16,185 images in the dataset, representing 196 different car classifications. The data is divided into 8,144 training images and 8,041 testing images, with about a 50-50 ratio between the two classes. Typically, classes are organized by Make, Model, and Year, such as 2012-Tesla-Model-S or 2012-BMW-M3-

coupe. Each image in the dataset has also a bounding-box output value as an ideal reference that suits our requirement.

*Pre-Processing.* We considered a total of 8,041 training images and passed them through two preprocessing stages. At first image augmentation was done to simulate challenging conditions which the real-time traffic video might face. The applied augmentations include: rotate, shift, flip, varying contrast, blur, and salt and pepper noise. After augmentation, label-encoding and training-validation split are done. In this case, we made an 80-20 split. After the splitting, the model is trained and tuned.

*Transfer Learning (TL).* A pre-trained model (NASNet-Mobile) as the backbone architecture of the proposed model ensures optimised training. Unlike the isolated learning paradigm, Transfer learning allows extending the pre-learned features to adequately address the new related challenges. Particularly, an average pooling layer usually can extract the pretrained models edge detection capability. From the final layer of shape  $(10 \times 10 \times 1056)$ , an average pooling layer is thus added followed by a group of fully connected dense layers and dropout layers. Finally the output layers identifies the object and generates the bounding box coordinates. Thus, our model was pre-trained with over fourteen million images from the ImageNet dataset, which is now capable of categorising images into over 1000 different classes with transfer learning ability. As a result, it has accumulated a library of rich feature sets for a wide variety of classes.

*Hyper-parameters and Tuning.* The training hyper-parameters are given in Table 1. Finally, the parameters with the best accuracy have been chosen

after several trials and errors. The optimizer that suits best for the VLP detection is Stochastic gradient descent(SGD). We have also tweaked several parameters of the optimiser for our dataset and defined early stopping to reduce the training time. Additionally, Reduced Learning Rate functionality has been used to further expedite the training process.

Table 1: Comparison of the training hyper-parameters

Model	Ours (BLPnet)		Onim <i>et al.</i> [17]		Zou <i>et al.</i> [10]	Hendry & Chen [11]	Li <i>et al.</i> [24]
Parameters	Vehicle	VLP	Vehicle	VLP	VLP	VLP	VLP
Backbone	NASNet Mobile	InceptionV3	Darknet	Darknet	MobileNetV3	Darknet	-
Classes	1	1	4	1	37	60	37
Batch size	32	64	32	64	-	-	32
Image Shape	300 × 300	200 × 200	224 × 224	128 × 128	152 × 56	256 × 256	24 × 24
Optimizer	SGD	Adam	Adam	Adam	SGD	Adam	Adam
Epochs	300	300	100	3500	-	600	-

### 3.2. VLP Detection with Inception-v3

We have also extended the Inception-v3 DNN architecture and employed it as the backbone of the second phase process of BLPnet for VLP detection as illustrated in Fig. 3. Inception-v3 is a CNN designed from the Inception family that transports label-information to a lower level of the network using label-smoothing, factorised  $7 \times 7$  convolutions, an auxiliary classifier, and batch-normalization for layers in the side head. Inception architecture being 42 layers deep has 2.5 times lower computational cost than that of GoogLeNet and can function well even when memory and computational budgets were limited [25].

We have used an annotated dataset of 1500 training and 300 validation images to train our model. From real-world video footage taken on roadways

in Dhaka, Bangladesh, with varying road conditions, including high traffic congestion, the VLP were detected with reasonably higher accuracy (see Sec. 4). The training began with a number of iterations set at 6000. The average loss did not diminish significantly after 2000 iterations, and after each 1000 cycles, the training was capable of taking weight backup. To reduce training duration, we thus used early stopping.

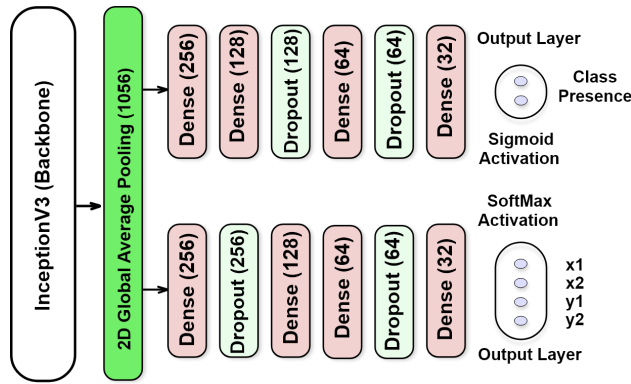


Figure 3: License Plate Bounding-box detector of the proposed ALPR system

### 3.3. A New Bengali-OCR Engine

This step recognised characters in the extracted VLP from the previous step. Similar to [26], we addressed the character recognition as an object recognition problem. By treating characters as objects, the character segmentation and recognition steps are integrated together that consists of a total 5 convolutional 2D layers with 16, 32, 64, 128 and 512 nodes. Each of them includes a preceding max-pooling layer with a pool size of 2 and a dropout layer with a drop rate of 20%. The dropout layers were used to prevent the model from over-fitting. The kernel size of 2 is considered with necessary padding. Relu activation function is used for all the backbone lay-

ers. Finally, a global-average pooling layer is included before the output layer followed by two dense layers. Two important considerations of this model are the conditional use of de-blurring filter and intensity inhomogeneity invariant segmentation of the character.

Blurring is known to be a key challenge in VLP recognition resulting from wrong focusing or vehicle’s motion that requires restoration of the blurred images for a higher accuracy in character recognition. A set of filters like Wiener filter, Total Variation (TV) deblurring, Haar deblurring and a combination of both is considered for restoring any blurred image to its estimated original version. For an input image,  $Im[n]$ , let the output of the filter is  $x[n]$  as in (1a), where  $G(z)$  is the filter function,  $N$  is the number of past taps with coefficient  $a$ ,  $s[n]$  is the reference signal, and  $e[n]$  is the residual error. The criteria to minimize the mean squared error (MSE) for the coefficient is defined in (1b), where  $E[.]$  is the expectation operator. On the other hand, Haar deblurring [27] uses a deconvolution filter and reduce the MSE as in (2), where  $I(i, j)$  is the expected and  $G(i, j)$  is the desired deblurred images. In our model, we have designed a conditional deblurring process invoked when not enough number of characters are detected in the OCR. An iterative approach is employed for this process with a varying threshold based on the Fast-Iterative Shrinkage Thresholding Algorithm (FISTA) [28] in the VLP image.

$$x[n] = \sum_{i=0}^N a_i \times Im[n - 1] \quad (1a)$$

$$a_i = \operatorname{argmin} (E [e^2[n]]) \quad (1b)$$

$$MSE = \frac{1}{m \times n} \sum_{i=0}^{m-1} \sum_{j=0}^{n-1} [I(I, J) - G(i, j)]^2 \quad (2)$$

Additionally, we have considered the intensity inhomogeneity invariant segmentation of the characters. Thus, we extracted the characters from the VLP with two segmentation models: Chan & Vese (CV) model and Region-Scalable Fitting (RSF) model (see Table 5 in Sec. 4). As most of the images for VLP have very high contrast, CV model performed well in approximating the intensities of the foreground or object and background. In case of intensity inhomogeneity, CV model failed to segment the characters, where RSF model was used.

The complete architecture is illustrated in Fig. 4. The output layer contains 60 classes to capture the total number of Bengali alphabets and digits. The output layer uses *Softmax* as an activation function. We have also used CMATERdb version 3.1.2 for training the alphabets for the digits. A total alphabet-images of 15000 and digits of 500 have been split as follows: 9900 images for training, 2600 images for validation, and 3000 images for testing.

The images are then augmented so that the model can identify images on non-ideal conditions. The following augmentations are considered: (i) 10% shift in left and 10% shift in right; (ii) 10% shift in vertical and 10% shift in horizontal; (iii) 7.5° rotation in left and 7.5° in right; (iv) zoom range 20%; and, (v) Shear range 20%. Besides, each character illustrated in Fig. 5 is resized to  $16 \times 16$  after segmentation before passing through the network. As a result, this network can work with variable size characters.

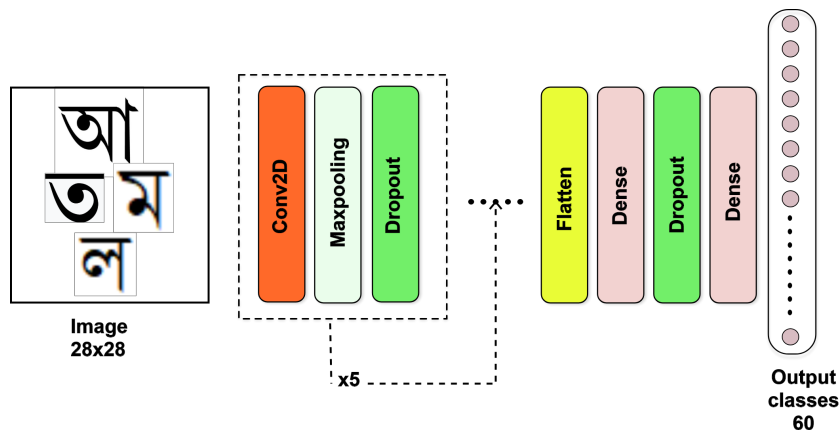


Figure 4: The newly developed OCR engine for BLPnet

Type	Characters
Alphabets	'অ', 'আ', 'ই', 'ঈ', 'ঊ', 'ঋ', 'ঌ', 'এ', 'ঐ', 'ও', 'ঔ', 'ক', 'খ', 'গ', 'ঘ', 'ঙ', 'চ', 'ছ', 'জ', 'ঝ', 'ঞ', 'ট', 'ঠ', 'ড', 'ঢ', 'ণ', 'ত', 'থ', 'দ', 'ধ', 'ন', 'প', 'ফ', 'ব', 'ভ', 'ম', 'য', 'র', 'ল', 'শ', 'ষ', 'স', 'হ', 'ড়', 'ঢ়', 'য়', 'ৎ', 'ং', '্', 'ঁ', 'া'
Digits	'০', '১', '২', '৩', '৪', '৫', '৬', '৭', '৮', '৯'

Figure 5: Bengali character classes for the OCR training

#### 4. Results and Analysis

We now present the performance of the proposed BLPnet model for the ALPR system, and compare its performance with some related models: Li *et al.* [24], Hendry & Chen [11], Zou *et al.* [10], and Onim *et al.* [17]. This section starts with the analysis of total learnable parameters of the model followed by the results discussed in three main parts, namely, for vehicle detection, VLP detection and finally, for the OCR and word-mapping.

#### 4.1. Total Learnable Parameters

A dense layer with  $m$  input nodes and  $n$  output nodes will have a total of  $(n + 1) \times m$  learnable parameters. The pooling layers and dropout layers does not learn anything. For convolutional layers with  $p$  feature maps in input and  $q$  feature maps as output having a filter size of  $i \times j$  will have a total learnable parameters of  $(i \times j \times p + 1) \times q$ . The distribution of trainable parameters for bounding box detector across the network is noted in Table. 2. The total number of trainable parameters is calculated as shown in Equation. (3). Similarly, Table. 3 shows the trainable parameters for our OCR engine. Here *Layers* denotes the name and operation of added layers, *Shape* denotes the input shape of tensors for that particular layer and finally the trainable parameter for that layer.

Table 2: Trainable parameters for bounding box detector

<b>Layers</b>	<b>Shape</b>	<b>Trainable Parameters</b>
Global_AveragePooling2D	(None, 1056)	0
Dense	(None, 256)	270592
Dense	(None, 256)	270592
Dense	(None, 128)	32896
Dropout	(None, 256)	0
Dropout	(None, 128)	0
Dense	(None, 128)	32896
Dense	(None, 64)	8256
Dense	(None, 64)	8256
Dropout	(None, 64)	0
Dropout	(None, 64)	0
Dense	(None, 32)	2080
Dense	(None, 32)	2080
Dense	(None, 2)	66
Dense	(None, 4)	132
<b>Total</b>		<b>627k</b>

Table 3: Trainable parameters for OCR engine

Layers	Shape	Trainable Parameters
Conv2D	(None, 63, 63, 16)	80
MaxPooling2D	(None, 31, 31, 16)	0
Dropout	(None, 31, 31, 16)	0
Conv2D	(None, 30, 30, 32)	2080
MaxPooling2D	(None, 15, 15, 32)	0
Dropout	(None, 15, 15, 32)	0
Conv2D	(None, 14, 14, 64)	8256
MaxPooling2D	(None, 7, 7, 64)	0
Dropout	(None, 7, 7, 64)	0
Conv2D	(None, 6, 6, 128)	32896
MaxPooling 2D	(None, 3, 3, 128)	0
Dropout	(None, 3, 3, 128)	0
Conv2D	(None, 2, 2, 256)	131328
MaxPooling 2D	(None, 1, 1, 256)	0
Dropout	(None, 1, 1, 256)	0
Flatten	(None, 256)	0
Dense	(None, 256)	65792
Dense	(None, 512)	131584
Dropout	(None, 512)	0
Dense	(None, 60)	25650
<b>Total</b>		<b>397K</b>

$$\begin{aligned}
N_{detector} &= 2 \times ((1056 + 1) \times 256 + (256 + 1) \times 128 + (128 + 1) \times 64 \\
&\quad + (64 + 1) \times 32 + (32 + 1) \times 2) \\
&= 627k
\end{aligned} \tag{3}$$

#### 4.2. Vehicle Detection

We trained the vehicle bounding-box model for vehicle detection for 1000 epochs with early stopping employed to stop the model training if the accuracy improvement is negligible. The hardware specification to train the

model is: Tesla K80 2496 CUDA cores GPU with 12 GB GDDR5 VRAM, Processor @2.3Ghz (4 core, 8 threads), and RAM of 48 GB.

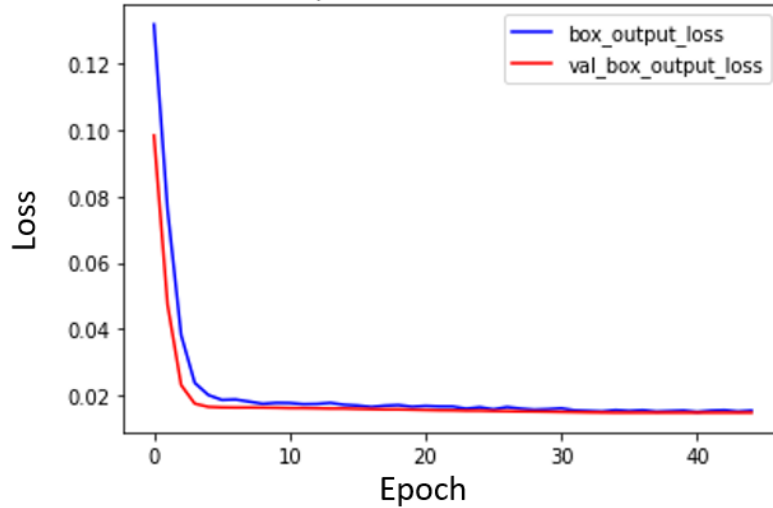
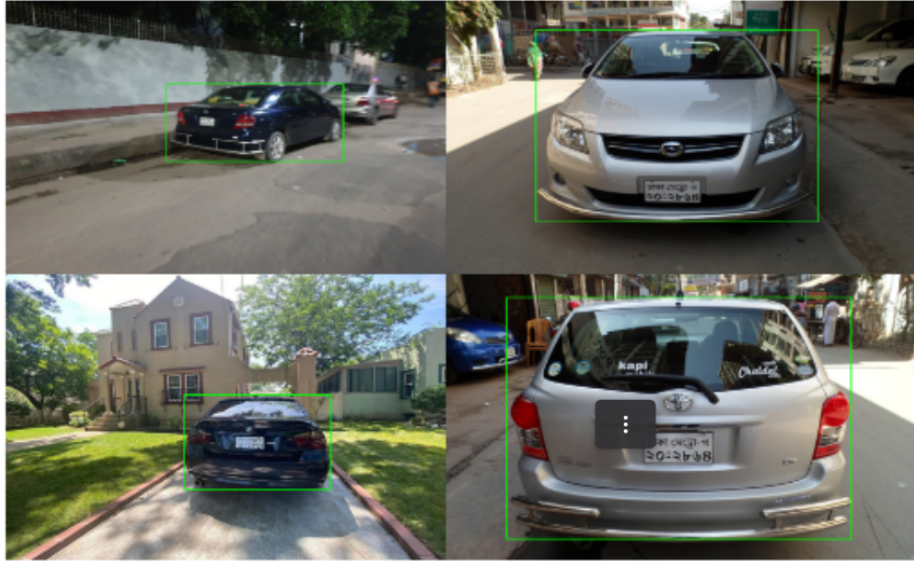


Figure 6: Loss vs Epoch curve for the first 50 epochs

We chose the criteria for our evaluation matrices of bounding-box coordinates to be MSE and accuracy. From the loss vs epoch curve in Fig. 6, we observe that the model can quickly converge to a lower loss value. After a while, the improvement gets very slow. The best training loss and MSE of bounding-box were 0.0130 and 0.0155, respectively and the validation loss and MSE were 0.0148 and 0.0152, respectively. Overall training parameters with their respective epochs is presented in Table 4. We observe in this table that after 300 epochs, the rate of change in loss and accuracy is becoming stable. Compared to the YOLO model, the hyper-parameters were kept similar as shown earlier in Table 1. All these observations suggest that the our proposed model would effectively detect the vehicles in the input video clips. The final predicted output of the model applied in random vehicles is shown



(a) Detected vehicles (marked with green bounding-boxes)



(b) VLP detection (marked with blue-colour bounding box)

Figure 7: Example of detected vehicles and VLP from real-time captured video footage with different orientations of the vehicles

in Fig. 7a with successful demarcation of green boxes.

Table 4: Performance of vehicle detection with bounding-box

Epochs	Loss	Box	Class	Box	Class	Validation Loss	Validation	Validation	Validation
		Output Loss	Output Loss	Output MSE	Output Accuracy		box Output Loss	class Output Loss	box Output MSE
50	0.0056	0.0176	0.0059	0.0176	75.59	0.0057	0.0175	0.0057	0.0175
100	0.0056	0.0171	0.0058	0.0171	85.89	0.0056	0.0140	0.0057	0.0140
150	0.0056	0.0169	0.0058	0.0169	89.19	0.0055	0.0138	0.0056	0.0138
200	0.00569	0.0173	0.0057	0.0173	90.55	0.0055	0.0175	0.0055	0.0175
250	0.00569	0.0176	0.0056	0.0176	94.74	0.0054	0.0175	0.0055	0.0175
300	0.00569	0.0176	0.0053	0.0176	96.99	0.0055	0.0175	0.0054	0.0175
350	0.00569	0.0176	0.0052	0.0176	97.02	0.0055	0.0175	0.0054	0.0175
400	0.00582	0.0130	0.0050	0.0155	97.05	0.0056	0.0148	0.0058	0.0152

### 4.3. VLP Detection

Our model was evaluated using both real-time and pre-recorded video clips. Table 1 shows the hyper-parameters used to train the network. Our model did not over-fit due to the use of adequate *dropout* and *pooling* layers, and thus, it took little time to train and converge to an optimum detection level. During the evaluation, the performance of the model was monitored in real-time.

Our algorithm successfully detected VLP as a few examples are illustrated in Fig. 7b, where VLP is marked with blue bounding box. A VLP was detected from varying orientation of the detected vehicle and at that time, 17 frames per second processing speed was maintained on average. Such accurate detection was observed for all the testing video clips with resolution  $1920 \times 1080$  and frames per second (*fps*) is of 15 and 20.

Similar to the vehicle detection with bounding box (Sec. 3.1), the VLP detection training loss and MSE of bounding-box were 0.013 and



Figure 8: Example of input and outputs of the newly developed OCR engine (From *top*, input images in *first row*, CV-segmented images in *second row*, LSF-segmented images in *third row*, and OCRs and word-mapping in *fourth row*)

0.016, respectively and the validation loss and MSE were 0.015 and 0.015, respectively. No false-positive detection was recorded during the process which justifies the effectiveness of previous phase.

#### 4.4. Character Recognition

The overall procedure can be broken down into three steps. First the preprocessing step, where the image is filtered based on the sharpness. Later in character segmentation, the fast active contour model segments the characters as objects. Finally, the character recognition followed by a word mapping. Here, for each group of key characters recognised, a predefined word is mapped for them. Our model's generated character output is shown in Fig. 8.

Table 5: OCR performance for the CV and RSF based segmented characters

Segmentation Model	No of characters extracted	Accuracy of OCR (in %)	Time taken for OCR (in seconds)	Time taken for Tesseract (in seconds)
CV model	4	90	0.302	0.402
	5	83	0.395	0.548
	6	81	0.432	0.701
	8	80	0.502	0.705
RSF model	4	95	0.256	0.402
	5	93	0.312	0.548
	6	90	0.333	0.701
	8	89	0.398	0.705

Table 6: Average testing accuracy in characters recognition applications

Model	Accuracy	Recognising object
Hendry & Chen [11]	78.2%	VLP & characters (English)
Zou <i>et al.</i> [10]	79.5%	Blurry text recognition (English)
Onim <i>et al.</i> [17]	90.51%	VLP (Bengali)
<b>BLPnet (proposed)</b>	<b>95.0%</b>	Real-time VLP & characters (Bengali)

Our proposed OCR engine demonstrated reasonably better accuracy as it treated the characters as objects. The accuracy varies from 80% to 95% based on the number of characters extracted. The time it takes to extract a character varies between 0.302 to 0.502 seconds. The model is weak against some vowel pairs. This weakness was tackled successfully with word mapping (see Fig. 8). Detailed performance analysis is given in Table 5. The accuracy decreases with the increase in number of characters. A comparison with related OCR engines is shown in Table 6. The other performance of the proposed model is also compared with the other prominent models in Table 7. Considering the nullified False-Positives, lower computational complexity, reduced trainable parameters, and reasonably higher accuracy, the proposed

Table 7: Comparison of features of the ALPR systems

Model	VLP False-Positive Detection	Character rotational invariant?	Trainable parameters ( <i>Million</i> )	Processing time ( <i>s</i> )	Hardware
Hendry & chen [11]	Unknown	no	8.8	0.8 – 1.0	Core i7 Nvidia GTX 970 4GB GPU
Li <i>et al.</i> [24]	Heuristically minimized with CNN	no	1.0	2.0 – 3.0	Core i5 Nvidia Tesla k40c 4GB GPU
Zou <i>et al.</i> [10]	Unknown	yes	1.9	Unknown	Core i5 Nvidia Titan 12GB GPU
Onim <i>et al.</i> [17]	Eliminated using 2-phase detection	no	27	0.7 – 1.0	Core i5 Nvidia Tesla T4 6GB GPU
<b>BLPnet (Ours)</b>	<b>Eliminated using 2-phase detection</b>	<b>yes</b>	<b>0.97</b>	<b>0.32 – 0.52</b>	<b>Core i5 Nvidia Tesla k80 6GB GPU</b>

model has demonstrated a higher potential for a real-time ALPR application.

## 5. Conclusion

The development of an ALPR system is a timely requirement for modern transportation services. However, despite being the sixth largest population around the world [2], no significant progress can be tracked in the Bengali language countries or states for the ALPR system addressing their inadequate road-safety measures and poor traffic management. To this end, we have presented a computationally efficient and reasonably accurate BLPnet model for a new ALPR system. The model is designed to efficiently and correctly return the VLP number by considering a three-phase top-to-bottom approach. This means, the model starts from detecting the vehicle first, and then any possible VLP followed by the recognition of characters in the VLP.

This consideration is observed to be more effective with lower-computational time and accuracy than the prominent ALPR systems.

Moreover, the model generates the actual license number of the vehicle from the recognized characters using our simple, yet effective mapping algorithm with a set of predefined cases of registration area-codes. The model also performed well without compromising accuracy to tackle challenging conditions that cause rotated, blurry or noisy frames at the input. The preliminary results with the reasonably faster and accurate performance of the model suggest that it would be promising for the real-time ALPR application with a continuing development in future.

## References

- [1] S. Du, M. Ibrahim, M. Shehata, W. Badawy, Automatic license plate recognition (alpr): A state-of-the-art review, *IEEE Transactions on circuits and systems for video technology* 23 (2) (2012) 311–325.
- [2] What are the top 200 most spoken languages? (Feb 2021).  
URL <https://www.ethnologue.com/guides/ethnologue200>
- [3] O. Bulan, V. Kozitsky, P. Ramesh, M. Shreve, Segmentation-and annotation-free license plate recognition with deep localization and failure identification, *IEEE Transactions on Intelligent Transportation Systems* 18 (9) (2017) 2351–2363.
- [4] Z. Xu, W. Yang, A. Meng, N. Lu, H. Huang, C. Ying, L. Huang, Towards end-to-end license plate detection and recognition: A large dataset and

- baseline, in: *Computer Vision – ECCV 2018*, Springer International Publishing, Cham, 2018, pp. 261–277.
- [5] R. Laroca, E. Severo, L. A. Zanlorensi, L. S. Oliveira, G. R. Gonçalves, W. R. Schwartz, D. Menotti, A robust real-time automatic license plate recognition based on the YOLO detector, in: *International Joint Conference on Neural Networks (IJCNN)*, 2018, pp. 1–10. doi:10.1109/IJCNN.2018.8489629.
- [6] W. Wang, J. Yang, M. Chen, P. Wang, A light cnn for end-to-end car license plates detection and recognition, *IEEE Access* 7 (2019) 173875–173883. doi:10.1109/ACCESS.2019.2956357.
- [7] S. M. Silva, C. R. Jung, A flexible approach for automatic license plate recognition in unconstrained scenarios, *IEEE Transactions on Intelligent Transportation Systems* (2021) 1–11doi:10.1109/TITS.2021.3055946.
- [8] J. Zhuang, S. Hou, Z. Wang, Z.-J. Zha, Towards human-level license plate recognition, in: *Proceedings of the European Conference on Computer Vision (ECCV)*, 2018.
- [9] Z. Huang, Z. Pan, B. Lei, Transfer learning with deep convolutional neural network for sar target classification with limited labeled data, *Remote Sensing* 9 (9) (2017) 907. doi:10.3390/rs9090907.  
URL <http://dx.doi.org/10.3390/rs9090907>
- [10] Y. Zou, Y. Zhang, J. Yan, X. Jiang, T. Huang, H. Fan, Z. Cui, A robust license plate recognition model based on bi-lstm, *IEEE Access* 8 (2020) 211630–211641.

- [11] Hendry, R.-C. Chen, Automatic license plate recognition via sliding-window darknet-yolo deep learning, *Image and Vision Computing* 87 (2019) 47–56. doi:<https://doi.org/10.1016/j.imavis.2019.04.007>.
- [12] M. S. Al-Shemarry, Y. Li, S. Abdulla, An efficient texture descriptor for the detection of license plates from vehicle images in difficult conditions, *IEEE transactions on intelligent transportation systems* 21 (2) (2019) 553–564.
- [13] A. Bochkovskiy, C. Wang, H. M. Liao, Yolov4: Optimal speed and accuracy of object detection, *CoRR* abs/2004.10934 (2020). arXiv:2004.10934.  
URL <https://arxiv.org/abs/2004.10934>
- [14] G.-S. Hsu, J.-C. Chen, Y.-Z. Chung, Application-oriented license plate recognition, *IEEE Transactions on Vehicular Technology* 62 (2) (2013) 552–561. doi:10.1109/TVT.2012.2226218.
- [15] S. Montazzolli, C. Jung, Real-time brazilian license plate detection and recognition using deep convolutional neural networks, in: 2017 30th SIBGRAPI Conference on Graphics, Patterns and Images (SIBGRAPI), 2017, pp. 55–62. doi:10.1109/SIBGRAPI.2017.14.
- [16] H. Li, P. Wang, C. Shen, Toward end-to-end car license plate detection and recognition with deep neural networks, *IEEE Transactions on Intelligent Transportation Systems* 20 (3) (2019) 1126–1136. doi:10.1109/TITS.2018.2847291.

- [17] M. S. H. Onim, M. I. Akash, M. Haque, R. I. Hafiz, Traffic surveillance using vehicle license plate detection and recognition in bangladesh, in: 2020 11th International Conference on Electrical and Computer Engineering (ICECE), 2020, pp. 121–124. doi:10.1109/ICECE51571.2020.9393109.
- [18] A. Majumdar, Bangla basic character recognition using digital curvelet transform, Journal of pattern recognition Research 2 (1) (2007) 17–26.
- [19] M. Hasnat, M. R. Chowdhury, M. Khan, et al., Integrating bangla script recognition support in tesseract ocr (2009).
- [20] A. S. A. Rabby, S. Haque, S. Islam, S. Abujar, S. A. Hossain, Bornonet: Bangla handwritten characters recognition using convolutional neural network, Procedia computer science 143 (2018) 528–535.
- [21] L. Bai, Y. Zhao, X. Huang, A cnn accelerator on fpga using depthwise separable convolution, IEEE Transactions on Circuits and Systems II: Express Briefs 65 (10) (2018) 1415–1419.
- [22] J. Deng, W. Dong, R. Socher, L.-J. Li, K. Li, L. Fei-Fei, Imagenet: A large-scale hierarchical image database, in: 2009 IEEE Conference on Computer Vision and Pattern Recognition, 2009, pp. 248–255. doi:10.1109/CVPR.2009.5206848.
- [23] J. Krause, M. Stark, J. Deng, L. Fei-Fei, 3d object representations for fine-grained categorization, in: 4th International IEEE Workshop on 3D Representation and Recognition (3dRR-13), Sydney, Australia, 2013.

- [24] H. Li, P. Wang, M. You, C. Shen, Reading car license plates using deep neural networks, *Image and Vision Computing* 72 (2018) 14–23. doi:<https://doi.org/10.1016/j.imavis.2018.02.002>.
- [25] C. Szegedy, V. Vanhoucke, S. Ioffe, J. Shlens, Z. Wojna, Rethinking the inception architecture for computer vision, in: *Proceedings of the IEEE conference on computer vision and pattern recognition*, 2016, pp. 2818–2826.
- [26] C. Henry, S. Y. Ahn, S.-W. Lee, Multinational license plate recognition using generalized character sequence detection, *IEEE Access* 8 (2020) 35185–35199. doi:[10.1109/ACCESS.2020.2974973](https://doi.org/10.1109/ACCESS.2020.2974973).
- [27] T. D. Do, X. Cui, T. H. B. Nguyen, H. Kim, V. H. Nguyen, Blind deconvolution method using omnidirectional gabor filter-based edge information, *CoRR abs/1905.01003* (2019). arXiv:[1905.01003](https://arxiv.org/abs/1905.01003).  
URL <http://arxiv.org/abs/1905.01003>
- [28] A. Beck, M. Teboulle, A fast iterative shrinkage-thresholding algorithm for linear inverse problems, *SIAM Journal on Imaging Sciences* 2 (1) (2009) 183–202. arXiv:<https://doi.org/10.1137/080716542>, doi:[10.1137/080716542](https://doi.org/10.1137/080716542).  
URL <https://doi.org/10.1137/080716542>